Science of the Total Environment 454–455 (2013) 328–336

Contents lists available at SciVerse ScienceDirect

Science of the Total Environment

journal homepage: www.elsevier.com/locate/scitotenv

Monitoring PAH contamination in water: Comparison of biological and physico-chemical tools

A. Bourgeault [1,*], C. Gourlay-Francé

Cemagref, UR HBAN, Parc de Tourvoie, BP 44, 92163 Antony, France
FIRE FR-3020, 4 Place Jussieu, 75005 Paris, France

HIGHLIGHTS

- PAH contamination was monitored by deploying mussels and SPMDs over 11months along the Seine River.
- 5–6 ring PAHs which could not be quantified in spot samples, were measured in SPMDs.
- PAH concentrations in the mussels decreased during spawning.
- Temporal variation of bioaccumulated PAH may originate from a decrease of the mussels' metabolism during spawning.
- Biodynamic model was allowed to explain the bioaccumulation.

ARTICLE INFO

Article history:
Received 3 January 2013
Received in revised form 4 March 2013
Accepted 4 March 2013
Available online 2 April 2013

Keywords:
Polycyclic Aromatic Hydrocarbons
Bioaccumulation
Water
Bioavailability
Semi-Permeable Membrane Device
Zebra mussel

ABSTRACT

The suitability of biological methods and chemical-based passive samplers to determine exposure to PAHs was tested by deploying zebra mussels and SPMDs along the Seine River over 11 months. The concentration of 13 PAHs was analyzed every month in both water and mussels. The sum of the PAH concentrations in mussels, initially at 299 ng $g^{-1}_{dry\ wt}$, reached 2654, 3972 and 3727 ng g^{-1} at the end of exposure in the three sampling points taken through the river. The respective SPMD-available concentrations of TPAHs reached 9, 52 and 34 ng L^{-1}. Results showed seasonal variations of total PAH concentrations in the mussels, characterized by a decrease during spawning. The non-achievement of steady state concentration that was observed in mussels may be accounted for by the temporal variation of environmental concentrations. Thus, a bioaccumulation model based on kinetic rather than simple equilibrium partitioning was found to be more appropriate to describe PAH content in mussels. Moreover, biodynamic kinetic modeling proved useful to better understand the uptake and loss processes of pyrene. It clearly shows that these processes are markedly influenced by the biological state of the zebra mussels. The most realistic hypothesis is that the temporal variation of the biodynamic parameters may originate from a decrease of the mussels' metabolization of PAHs during spawning. Since SPMD passive samplers cannot integrate such biological factors, they are poor predictors of PAH bioavailability in mussels.

1. Introduction

The European Water Framework Directive (2000/60/EC) requires the evaluation of the chemical status of water bodies. This chemical evaluation is based on the measurement of priority substances listed in the WFD and the comparison of water concentrations with Environmental Quality Standards (EQSs). Polycyclic Aromatic Hydrocarbons (PAHs), which are included in these "priority substances", are of particular concern in aquatic ecosystems under urban pressure. As regards to PAHs, the mean annual EQSs in raw water are respectively 300, 50, 3 and 0.2 ng L^{-1} for fluoranthene, benzo[a]pyrene, the sum of benzo[b]fluoranthene and benzo[k]fluoranthene, and the sum of indeno(1,2,3-cd)pyrene and benzo[g,h,i]perylene. These very low EQSs require powerful analytical methods. Moreover, spot water sample analysis is a poor representative of actual contamination because of temporal variability, and it does not really inform on the potential biological impact of the contaminants since their bioavailability is not taken into account. Hence, several alternatives have been proposed over the past few years, such as biomonitoring and passive sampling techniques (Blasco and Picò, 2009).

Semi-Permeable Membrane Devices (SPMDs) (Huckins et al., 1993) are the most commonly used integrative passive samplers

* Corresponding author at: Laboratoire Interdisciplinaire sur l'Organisation Nanométrique et Supramoléculaire (LIONS), CEA de Saclay, 91191 Gif-sur-Yvette, France. Tel.: +33 1 69 08 67 65.
E-mail address: bourgeault@ensil.unilim.fr (A. Bourgeault).
[1] Present address: Laboratoire Interdisciplinaire sur l'Organisation Nanométrique et Supramoléculaire (LIONS), CEA de Saclay, 91191 Gif-sur-Yvette, France.

0048-9697/$ – see front matter © 2013 Elsevier B.V. All rights reserved.
http://dx.doi.org/10.1016/j.scitotenv.2013.03.021

for hydrophobic organic compounds (HOC). The accumulation of organic contaminants in SPMDs and in molluscs has been extensively compared, especially in marine environments (see for example Gale et al., 1997; Booij et al., 2002; Boehm et al., 2005). Moreover, the ability of both materials to estimate water contamination has also been investigated (Booij et al., 2002; Verweij et al., 2004). From a meta-analysis of available data, Booij et al. (2006) conclude that SPMDs provide a more reliable estimate of water contamination, and suggest using SPMD sampling in long-term monitoring programs. Although similar trends are usually identified in mussels and SPMDs in terms of spatial variability, accumulation patterns differ. Indeed, not only do kinetics and thermodynamic parameters differ between the two, but mussels also accumulate particulate contaminants, unlike SPMDs.

The bioaccumulation of contaminants is also influenced by the organisms' physiology. Hence, in field monitoring, it is still challenging to dissociate the environmental factors from the physiological factors that both drive the contamination actually measured in organisms. For instance, Binelli et al. (2001) reported a PCB concentration for zebra mussels in pre-reproductive stage that was twice higher than the one measured in post-reproductive stage. In the meantime, PCB levels in the water had fluctuated, making it hard to attribute the variation of PCB bioaccumulation to the reproductive stage. Bruner et al. (1994) also showed that the uptake rate of benzo(a)pyrene was higher for high-lipid pre-spawning mussels than low-lipid post-spawning ones. However, it was not the case for less hydrophobic compounds like pyrene. The interpretation of biomonitoring data requires mechanistic models that explicitly describe bioaccumulation processes and their influencing factors. The biodynamic model, for instance, has been extensively used to describe bioaccumulation in aquatic organisms (Booij et al., 2006; Wang and Rainbow, 2008; Bayen et al., 2009). It takes into account the uptake of contaminants from both water and particles but also the elimination and growth rates of organisms. However, as a first estimation, the trophic pathway has usually been discarded from this model to describe the bioaccumulation of hydrophobic compounds (Bayen et al., 2009).

The aim of this study was to investigate the ability of biological tools and passive samplers to reflect the spatio-temporal variability of water PAH contamination in an urban river. This ecosystem was characterized by a chronic multi-contamination, most substances being in the order of magnitude of Environmental Quality Standards. Over one year, zebra mussels were transplanted to three sites along the Seine River, concomitantly with SPMDs. Water, SPMDs and transplanted mussels were sampled monthly and analyzed for PAH concentrations. The ability of SPMDs to evaluate water contamination was tested. We also investigated the contamination process of zebra mussels by PAHs during a complete biological cycle in order to relate the contamination of water to that of mussels.

2. Materials and methods

2.1. Study area and sampling

Zebra mussels (20–22 mm) were collected in October 2008 in the Meuse-Marne canal (France), pooled into 36 cages (25 mussels per cage) and submerged in water from the canal until transplantation the following day. Twelve cages were deployed at each of the three sites along the Seine River: Site 1 is located in the upper part of the basin (Marnay-sur-Seine) and the other two are situated downstream from the city of Paris (Bougival, Site 2 and Triel-sur-Seine, Site 3). Site 2 is subjected to diffuse urban pollution. Site 3 is located a few kilometers downstream from the discharge of the wastewater treatment plant Seine-Aval and is thus subjected to both diffuse urban sources and wastewater discharge. A full description of the physico-chemical characteristics of the water during the sampling period is available in Priadi et al. (2011).

Two standard SPMDs were deployed at each site at the same time as the mussels (91.4 cm long, 2.5 cm wide, 1 mL triolein for a total volume of 4.95 cm^3, Exposmeter AB, Trehôrningen, Sweden). These had previously been spiked in the laboratory with five deuterated PAHs that were to serve as performance reference compounds (PRCs) (i.e. acenaphtylene-d_8, fluorine-d_{10}, anthracene-d_{10}, fluoranthene-d_{10} and benzo(g,h,i)perylene-d_{12} from Dr. Ehrenstorfer, Germany). SPMDs were prepared and deployed as described in Gourlay-Francé et al. (2008).

Over an 11-month period, the three sites were visited once a month. Each month, one cage was sampled and kept in water from the site in a refrigerated container for various biological analyses in the laboratory. The two SPMDs on site were retrieved and replaced by two new ones that had been spiked with PRCs the day before. Retrieved SPMDs were gently wiped with soft paper, replaced in their original box and brought back to the laboratory for analysis and assessment of the monthly average concentration in PAHs. Each month, three additional SPMDs were used as field and laboratory blanks (Bourgeault et al., 2010). Water samples (2.5 L each) were collected in bottles heated at 400 °C prior to use for particulate and dissolved PAH measurements. Water was also sampled for physico-chemical analysis (DOC, POC, chlorophyll, pheopigment, *TSS*, AFDW). pH, conductivity and temperature were measured on site.

2.2. SPMDs and water treatment

In the laboratory, SPMDs were cleaned with soft paper, rinsed with demineralized water and wiped dry. SPMDs were put in amber glass bottles containing 250 mL of heptane (Picograde, LGC Promochem, Molsheim, France) and 100 μL of internal standard (5 mg L^{-1}) (i.e. naphthalene-d_8, acenaphthene-d_{10}, phenanthrene-d_{10}, chrysene-d_{12} and perylene-d_{12}). The bottles were shaken for 48 h at room temperature for PAH extraction. The extract was then concentrated and purified on Florisil cartridges (Silica cartridges Chromabond Macherey-Nagel, France). The cartridges had previously been conditioned with 4 mL of heptane/ethylacetate (94:6 v:v). Once the sample was in place, cartridges were eluted with 20 mL of heptane/ethylacetate. The sample was concentrated under N_2 flow and conditioned in 1 mL of heptane.

Water was filtered through a glass-fiber filter (GFF Whatmann) heated at 400 °C prior to use. An internal standard (50 μL of a 1 mg L^{-1} solution) was added to the filtrate. Filtered water was solid-phase extracted using Chromabond C18 cartridges (Macherey-Nagel, France). Three cartridges were used for each 2-liter sample of water. After that, 2 mL of methanol was added and cartridges were dried for 20 min using a vacuum pump. PAHs were eluted with 10 mL of DCM. The solution was then concentrated under N_2 flow. The sample was finally conditioned in 100 μL of heptane in a vial and kept at −18 °C until analysis.

The particles collected on the GFF were freeze-dried and weighed. Particulate PAHs were microwave-extracted in a 20 mL solution of DCM/methanol (90/10 v/v) spiked with 20 μL of a solution of internal standard (2.5 mg L^{-1}). The extract was then filtered through a GFF (pre-cleansed with acetone) and concentrated to obtain a final volume of 500 μL. The sample was purified through a silica cartridge (Florisil eluted with 20 mL heptane/ethylacetate 94/6) and concentrated under N_2 flow. Its volume was finally adjusted to 1 mL in heptane. A certified reference sediment material (HS-5 Harbour sediment Canada NRC-CNRS) was used to verify the method of extraction and analysis.

2.3. Mussel treatment

In the laboratory, dead mussels were counted and discarded. The filtration rates of mussels were assessed as described in Bourgeault et al. (2011). Mussels were then dissected. Fresh soft tissues and shells were weighed individually on 15 organisms. The condition index (CI) was calculated as the ratio between the wet weight of the soft tissues and the total weight of the mussel. Each month, soft tissues were freeze-dried, pooled on a site-by-site basis and reduced to a powder for lipid and PAH analysis.

0.5 g of tissues was microwave-extracted in 20 mL of heptane/acetone (50/50) (v/v) containing 20 μL of internal standard solution (PAH mix 13 at 5 mg L^{-1} in acetone; Dr. Ehrenstorfer, Germany). The extract was filtered, evaporated and purified on a Florisil column as detailed in Bourgeault et al. (2010). The final extract in 200 μL of heptane was kept at −18 °C until analysis. The method of extraction and analysis was validated using a certified reference mussel homogenate (IAEA-432).

Lipid content was determined following Bligh and Dyer's method described in Voets et al. (2006). The lipid content in dried mussel tissue (10 mg) was extracted using chloroform, methanol and purified water and separated by centrifugation. After acidification with H_2SO_4 and 15 min at 200 °C, this lipid content was measured by spectrophotometry at 340 nm, using tripalmitine as standard.

2.4. PAH analysis

PAHs were analyzed by gas chromatography–mass spectrometry (Thermo trace GC Ultra DSQII) in ion-monitoring mode. Target PAHs were those on the US EPA list: naphthalene, acenaphtene, acenaphtylene, fluorene, phenanthrene, anthracene, fluoranthene, pyrene, benzo(a)anthracene, chrysene, benzo(b)fluoranthene, benzo(k)fluoranthene, benzo(a)pyrene, indeno(1,2,3-cd)pyrene, dibenzo(a,h)anthracene and benzo(g,h,i)perylene. However, naphthalene, acenaphtene and acenaphtylene were excluded since these compounds had low recovery rates in the reference materials. Quantification limits, corresponding to the lowest concentration of the working range, were 0.01 ng μL^{-1} in the final extract for each PAH.

Particulate (C_{part}) and total dissolved ($C_{dissolved}$) PAH concentrations measured in water samples were both expressed in ng L^{-1}. Time-weighted average concentrations of truly dissolved PAHs ($C_{SPMD\text{-}available}$) were estimated from PAH and PRC concentrations in SPMDs, following Huckins et al. (2006). For each SPMD, one PRC with a dissipation rate between 30 and 70% was chosen for the correction of sampling rates. For all concentrations, the sum of the thirteen target PAHs is referred to below as TPAH.

3. Bioaccumulation modeling

First, the bioconcentration factor (*BCF*) and biota-sediment accumulation factor (*BSAF*) were calculated:

$$BCF = \frac{C_{org}}{C_{dissolved}} \quad (1)$$

$$BSAF = \frac{C_{org\_lip}}{C_{part\_OC}} \quad (2)$$

where C_{org} is the PAH concentration in the organism, $C_{dissolved}$ is the concentration in the water, C_{org_lip} is the lipid-adjusted concentration in the organism and C_{part_OC} is the POC-adjusted concentration in particles.

Second, we attempted to determine whether the biodynamic model was able to describe the relationship between water and mussel contamination. The biodynamic model describes PAH accumulation in organisms over time as follows (Wang and Rainbow, 2008):

$$\frac{dC_{org}}{dt} = k_u \cdot C_{dissolved} + AE \cdot IR \cdot C_{part} - (k_e + g) \cdot C_{org} \quad (3)$$

where t is the time of exposure (d), k_u is the uptake rate constant from the dissolved phase (L g^{-1} d^{-1}), *AE* is the assimilation efficiency of ingested PAHs (%), *IR* is the ingestion rate (g g^{-1} d^{-1}) which is defined as $TSS \times FR$, k_e is the efflux rate constant (d^{-1}) (which includes the rate constant for depuration via gills and feces and the biotransformation constant) and g is the growth rate constant of the animal (d^{-1}).

In order to apply the biodynamic model to the monthly data obtained in the present study, we hypothesized that environmental variables (i.e. *TSS* concentration, $C_{dissolved}$ and C_{part}) and physiological parameters (*FR* and g) are constant between t_{i-1} and t_i, but may vary from month to month. The PAH concentration in mussel tissues is thus described by the following equation, as detailed in a previous study (Bourgeault et al., 2011):

$$C_{org}(t_i) = C_{org}(t_{i-1}) \cdot e^{-(k_e+g)\cdot(t_i - t_{i-1})} + C_{org\_ss} \cdot \left(1 - e^{-(k_e+g)\cdot(t_i - t_{i-1})}\right) \quad (4)$$

where $C_{org\_ss} = \frac{k_u \cdot C_{dissolved} + AE \cdot TSS \cdot FR \cdot C_{part}}{k_e + g}$.

$C_{dissolved}$, C_{part}, *TSS*, *FR* and g were obtained by averaging the values measured between t_{i-1} and t_i. However, for the calculation of g we imposed $g \geq 0$. Indeed, we hypothesized that the PAH concentration in the gonads is similar to the overall concentration in mussel tissue, and that the expulsion of gamets during spawning, which actually leads to a loss of weight, does not modify the overall PAH concentration in mussels. *AE*, k_u and k_e values were obtained from the literature. Available data on the uptake and loss kinetics of PAH accumulation in zebra mussels is restricted to pyrene and B(*a*)P (Gossiaux et al., 1998; Fisher et al., 1993). Since B(*a*)P concentrations measured in mussels were low (2% of TPAHs on average) and non-quantifiable in several filtered water samples, the modeling investigation was limited to pyrene. Gossiaux et al. (1998) reported pyrene AEs of 91.5% and 58.3% for algae and sediment respectively. Fisher et al. (1993) determined an uptake rate constant (k_u) and an efflux rate constant (k_e) of 428 mL $g^{-1}_{wet\ wt}$ h^{-1} and 0.096 h^{-1} respectively for pyrene.

4. Results

4.1. Water contamination

The total dissolved concentration of the sum of the 13 PAHs in water over the whole year averaged 25, 126 and 63 ng L^{-1} at Sites 1, 2 and 3 respectively (Fig. 1 and Table 1). Dissolved TPAH and SPMD-available concentrations at Sites 2 and 3 were significantly higher than those at Site 1 (Kruskal–Wallis test, $p < 0.05$). As was previously observed in the same area a few years ago (Tusseau-Vuillemin et al., 2007), Site 2 was the most contaminated site all year round. This was attributed to the nearby industrial area located a few kilometers upstream from Site 2.

In almost all samples from Sites 2 and 3, 5–6 ring PAHs which could not be quantified in spot samples (water and particles), were measured in SPMDs (Table 1). SPMD-available concentrations were calculated from the PAH amount in SPMDs and PRC losses in all the exposed SPMDs. When total dissolved and labile PAH concentrations were quantified, SPMD-available concentrations were smaller than total dissolved ones in 75% of cases.

No temporal tendency was observed in the concentration of individual PAHs over the year.

Due to analytical troubles (mechanical failure of the GC–MS), particulate PAH samples, which were analyzed in the same analytical run, could not be analyzed satisfactorily over the first 5 months. Hence, PAH concentrations in particles were measured only for months 6 to 11. Particulate contamination was variable over the duration of exposure and similar from one site to the next: the mean sum of the 13 PAH concentrations in *TSS* was 21 ± 21 μg g^{-1}, 23 ± 16 μg g^{-1} and 20 ± 13 μg g^{-1} at Sites 1, 2 and 3 respectively (Table 1). The total particulate PAHs accounted for 86%, 63% and 76% of the contamination of the water column at Sites 1, 2 and 3 respectively.

The PAH concentrations of the most hydrophobic compounds (BbF + BkF and BghiP + IndP) exceeded EQSs at all three sites.

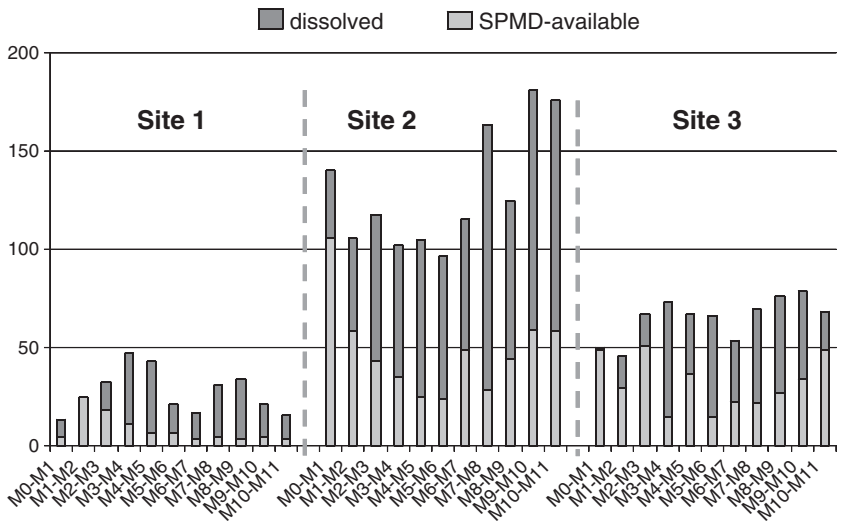

Fig. 1. Sum of the total dissolved concentrations of the 13 PAHs (light plus dark gray) and SPMD-available concentrations (light gray) measured each month at the three sites (ng L^{-1}).

4.2. Mussel physiology

The transplantation of mussels did not lead to a decrease of the condition index (CI) (Fig. S1) and mortality remained below 25% over the first 9 months of transplantation. At all three sites, soft tissues grew slightly in the spring, leading to a high CI, with a maximum in April. CI decreased at all three sites between April 22nd and June 9th, which was attributed to mussel spawning. The spawning period was verified by the measurement of the gonado-somatic index in the mussels transplanted concomitantly for another study (Michel et al., in press). In the summer, CI decreased at all three sites. A high mortality was observed in August at the two downstream sites (from 70% to 79%) and in September at Site 1 (88%). This sudden increase in mortality observed at all three sites may be explained by high water temperatures or low oxygen concentrations, or may result from a decline in the general health status of organisms as revealed one month earlier by the drop of the condition index. The filtration rate was higher for mussels exposed at Site 1 than at both downstream sites (Fig. S2). This could result from a lower food supply at Site 1, as detailed elsewhere (Bourgeault et al., 2011). The dry to wet tissue ratio and the lipid content in mussel tissue remained constant at all sites and throughout the exposure. The dry to wet tissue ratio was 0.12 ± 0.02 (n = 36) and the lipid weight accounted for 7.4 ± 0.6% of the dry weight (n = 36).

4.3. Mussel PAH contamination

Dibenzo[a,h]anthracene and benzo[g,h,i]perylene were never detected in mussel tissues.

Mussel tissues were more contaminated at the two downstream sites than at Site 1 (Fig. 2 and Table 1). The non-parametric tests (z-test) showed significant differences between Sites 1 and 2 throughout the 11 months of exposure ($p < 0.05$), except in February ($p > 0.09$). The difference between Sites 1 and 3 was less pronounced and was significant only half the time during the exposure. Over the 11-month exposure, the mussel TPAH contamination increased significantly at all three sites ($r^2 > 0.69$, $p < 0.02$). The decrease of TPAH concentrations in April was concomitant with spawning.

The TPAH concentrations measured in the present study (expressed on a wet basis) were one order of magnitude below the concentrations measured in zebra mussels deployed for one month in a highly contaminated area (Roper et al., 1997). Indeed, the TPAH concentrations reported by Roper et al. (1997) reached 6600 ng $g^{-1}_{\text{wet weight}}$, compared to a maximal concentration of 500 ng $g^{-1}_{\text{wet weight}}$ obtained at Site 2. By contrast, Binelli et al. (2010) reported TPAH concentrations that were 100 times lower in zebra mussels exposed ex-situ.

4.4. PAH distribution

The distribution between 3, 4 and 5–6 ring PAHs in the various matrices is given in Fig. S3. As expected, compounds with the lowest molecular weight (3-ring PAHs) were preferentially found in the dissolved phase (40–73% of PAHs, depending on the site), whereas those with the highest molecular weight (4, 5 and 6 rings) tended to be bound to particles. PAH distribution in mussels was found to be intermediate between those in the dissolved and the particulate phases — depending on the site, the proportion of 3-ring PAHs varied between 25 and 46%. In all matrices, 3-ring PAHs were proportionally more important at the upstream site (Site 1) than at Sites 2 and 3.

5. Discussion

5.1. Use of passive samplers for a better assessment of water contamination

The exchange rates for each PRC varied by a factor of 3 between sites each month, and by a factor of 10 over the year. This means that SPMD exposure conditions strongly influenced the kinetics of PAH accumulation. Hence, the comparison of PAH contents in SPMDs is not an appropriate proxy for water contamination, even in the same river or at the same place at different times. It is absolutely necessary to evaluate an SPMD-available PAH concentration in water from the accumulation of PAHs in SPMDs in order to be able to compare site contaminations.

No seasonal variation was noticed for any PAH. Hence, the PAH concentrations in water (SPMD-available, dissolved or total) for each individual PAH were averaged over the sampling period. As observed in Fig. 3, the SPMD-available PAH concentrations were highly correlated with the total ($r^2 = 0.71$) and dissolved ($r^2 = 0.89$) PAH concentrations. Since SPMDs simplify the sampling, in particular for highly hydrophobic compounds, the use of such passive samplers is of great interest to estimate water contamination. Nevertheless, the comparison with PAH EQSs is not straightforward, as the SPMD-available substances are only a fraction of the PAHs in raw water. Indeed, it has been verified that the SPMD-available PAH fraction is close to the freely dissolved one in various aquatic environments (Gourlay et al., 2005; Gourlay-Francé et al., 2008). The fraction of SPMD-available PAHs in water depends on their hydrophobicity (the more hydrophobic, the less SPMD-available), but also on the presence of organic matter in the water (the more concentrated the

Table 1
Dissolved, SPMD-available, particulate and bioaccumulated concentrations of the 13 PAHs over the whole year. The results are indicated for each site as minimum–maximum–average values. The frequency of detection is in parenthesis (n = 12 for dissolved concentrations, n = 11 for SPMD-available concentrations, n = 11 for bioaccumulated concentrations at Sites 1 and 3, n = 10 for bioaccumulated concentrations at Site 2, n = 6 for particulate concentrations). TPAH is the sum of the 13 PAHs.

		Fluorene	Phenanthrene	Anthracene	Fluoranthene	Pyrene	Benzo(a) anthracene	Chrysene
Dissolved ($ng\ L^{-1}$)	Site 1	1.7–49.4–11.8 (100%)	3.6–13.5–7.0 (100%)	0.1–1.2–0.5 (92%)	1.5–4.7–2.8 (100%)	0.8–4.6–2.0 (100%)	0.1–0.6–0.2 (67%)	0.1–0.8–0.2 (100%)
	Site 2	4.1–49.5–24.8 (92%)	9.5–46.8–24 (100%)	2.1–18.6–6.3 (100%)	11.3–101.5–29.5 (100%)	13.2–128.9–34.7 (100%)	1.3–7.5–3.0 (92%)	0.8–6.1–2.4 (100%)
	Site 3	1.5–31.9–13.9 (100%)	5.0–27.5–13.3 (100%)	0.8–4.7–2.4 (92%)	5.4–28.2–11.4 (100%)	5.9–49.5–16.5 (100%)	0.5–2.7–1.3 (92%)	0.4–3.7–1.2 (100%)
SPMD-available ($ng\ L^{-1}$)	Site 1	0.3–3.1–1.0 (100%)	0.8–9.1–2.8 (100%)	0.1–0.7–0.3 (100%)	0.9–6.8–2.2 (100%)	0.4–4.1–1.3 (100%)	0.0–0.2–0.1 (73%)	0.0–0.4–0.2 (100%)
	Site 2	1.3–5.3–2.5 (100%)	3.4–9.1–5.9 (100%)	1.0–3.3–1.8 (100%)	5.4–24.9–11.3 (100%)	8.9–54.5–19.2 (100%)	0.9–3.5–2.1 (100%)	0.8–3.2–1.7 (100%)
	Site 3	0.7–10.0–2.8 (100%)	1.7–16.2–5.4 (100%)	0.4–3.6–1.3 (100%)	0.9–11.7–5.7 (100%)	5.0–27.9–11.4 (100%)	0.3–3.7–1.4 (100%)	0.3–4.1–1.4 (100%)
Particulate ($\mu g\ g^{-1}$)	Site 1	0.07–1.90–0.64 (100%)	0.32–1.27–0.76 (100%)	0.02–0.09–0.05 (100%)	0.69–13.40–4.51 (100%)	2.09–41.81–14.08 (100%)	0.04–0.11–0.08 (100%)	0.07–0.14–0.11 (100%)
	Site 2	0.21–0.51–0.38 (100%)	0.73–2.21–1.38 (100%)	0.17–0.96–0.41 (100%)	1.66–11.36–4.82 (100%)	3.50–30.21–11.62 (100%)	0.26–0.73–0.56 (100%)	0.26–0.81–0.61 (100%)
	Site 3	0.23–0.58–0.37 (100%)	0.57–1.85–1.17 (100%)	0.10–0.27–0.20 (100%)	1.71–9.19–4.15 (100%)	4.08–24.85–10.87 –(100%)	0.19–0.46–0.35 (100%)	0.20–0.51–0.38 (100%)
Bioaccumulated in mussels ($ng\ gdw^{-1}$)	Site 1	9–40–18 (100%)	155–1075–494 (100%)	8–59–26 (100%)	25–590–271 (100%)	18–1016–481 (100%)	3–24–9 (100%)	4–40–14 (100%)
	Site 2	8–26–15 (100%)	155–994–564 (100%)	8–68–40 (100%)	30–795–428 (100%)	32–1456–689 (100%)	11–352–179 (100%)	11–348–161 (100%)
	Site 3	11–68–25 (100%)	155–999–568 (100%)	8–73–36 (100%)	30–770–384 (100%)	32–1560–689 (100%)	11–232–101 (100%)	11–287–117 (100%)

		Benzo(b)fluoranthene	Benzo(k)fluoranthene	Benzo(a)pyrene	Indeno(1,2,3-cd)pyrene	Dibenz(a,h)anthracene	Benzo(g,h,i)pérylene	THAP
Dissolved ($ng\ L^{-1}$)	Site 1	0.1–1.7–0.6 (33%)	0.1–0.6–0.3 (33%)	0.7–0.7–0.7 (8%)	0.1–1.1–0.4 (25%)	nd (0%)	0.1–1.1–0.4 (33%)	8.9–62.5–25.1
	Site 2	0.6–3.5–1.7 (58%)	0.2–1.4–0.8 (58%)	0.4–10.5–1.8 (92%)	0.1–3.1–0.9 (50%)	nd (0%)	0.2–2.0–0.7 (58%)	47.7–271.8–126.4
	Site 3	0.1–4.2–1.3 (50%)	0.2–1.5–0.6 (58%)	0.2–6.5–1.3 (92%)	0.1–3.5–1.1 (42%)	0.4–0.6–0.5 (17%)	0.2–2.3–0.7 (67%)	35.9–100.0–62.9
SPMD-available ($ng\ L^{-1}$)	Site 1	0.2–0.4–0.3 (73%)	0.0–0.2–0.1 (64%)	0.1–0.3–0.1 (45%)	0.1–0.1–0.1 (45%)	nd (0%)	0.1–0.2–0.1 (45%)	3.5–24.4–8.6
	Site 2	0.4–2.2–1.4 (100%)	0.1–0.9–0.5 (100%)	0.3–2.1–1.1 (100%)	0.1–0.5–0.3 (91%)	0.1–0.2–0.1 (45%)	0.1–0.8–0.4 (91%)	24.1–105.9–51.8
	Site 3	0.2–1.6–0.8 (100%)	0.1–0.6–0.3 (100%)	0.1–1.3–0.6 (100%)	0.1–0.2–0.1 (91%)	0.1–0.1–0.1 (27%)	0.1–0.7–0.3 (91%)	14.6–50.4–33.6
Particulate ($\mu g\ g^{-1}$)	Site 1	0.05–0.21–0.13 (100%)	0.03–0.11–0.05 (100%)	0.07–1.12–0.31 (100%)	0.04–0.15–0.10 (100%)	nd (0%)	0.09–0.15–0.11 (100%)	4–64–21
	Site 2	0.32–0.91–0.75 (100%)	0.16–0.51–0.40 (100%)	0.34–1.05–0.76 (100%)	0.25–0.70–0.57 (100%)	nd (0%)	0.26–0.81–0.59 (100%)	9–50–23
	Site 3	0.27–0.66–0.50 (100%)	0.11–0.34–0.24 (100%)	0.27–1.97–0.70 (100%)	0.20–0.48–0.37 (100%)	nd (0%)	0.22–0.49–0.39 (100%)	9–41–20
Bioaccumulated in mussels ($ng\ g_{dw}^{-1}$)	Site 1	4–32–14 (100%)	2–38–9 (100%)	4–32–15 (91%)	18–18–18 (10%)	nd (0%)	nd (0%)	327–2753–1391
	Site 2	16–255–159 (100%)	5–120–55 (100%)	74–149–103 (82%)	1–18–9 (20%)	nd (0%)	nd (0%)	329–4180–2425
	Site 3	16–183–72 (100%)	5–97–31 (100%)	41–124–53 (36%)	12–28–20 (63%)	nd (0%)	nd (0%)	329–3784–2099

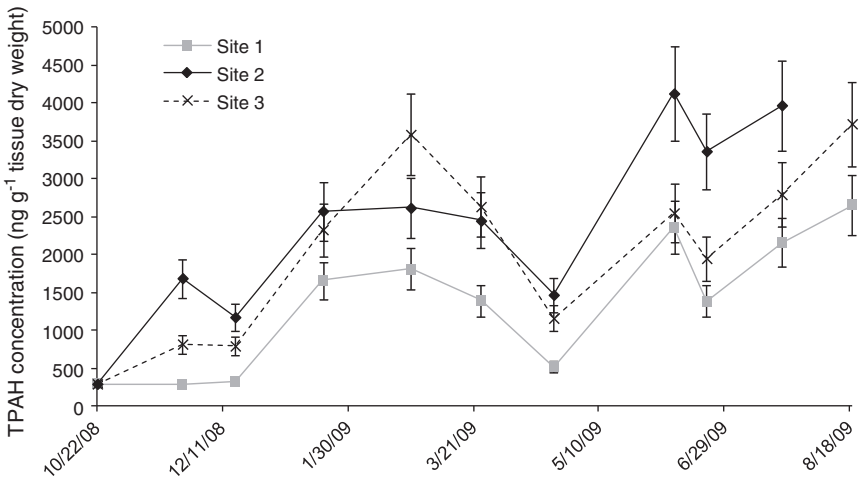

Fig. 2. Concentration of the sum of the 13 PAHs (TPAH) in mussel tissue transplanted to the three sites along the Seine River. Due to the limited availability of biological material, the PAH measurements in pooled mussel tissues were not replicated. The size of each pool (20–25 mussels) likely limited biological variability. Still, we considered a 15% variability based on Bervoets's study (Bervoets et al., 2004).

organic matter, the less SPMD-available the PAH). Hence, taking into account the concentration of organic matter in the water and the hydrophobicity of the compounds should improve the correlation between SPMD-available and raw concentrations.

Assuming that the partitioning between freely dissolved PAHs and PAHs bound to total organic matter remains constant over time, it should be possible to estimate C_{total} from $C_{SPMD\text{-}available}$ using the partitioning constant K_{TOC} (Allan et al., 2009).

$$C_{total} = C_{SPMD-bioavailable}(1 + K_{TOC}[TOC]) \quad (5)$$

where [*TOC*] is the total organic carbon concentration (i.e. the sum of dissolved and particulate organic carbon, expressed in mg L^{-1}).

The partitioning constant was evaluated based on Schwarzenbach et al. (1993):

$$\log K_{TOC} = 0.98 \log K_{OW} + 0.38. \quad (6)$$

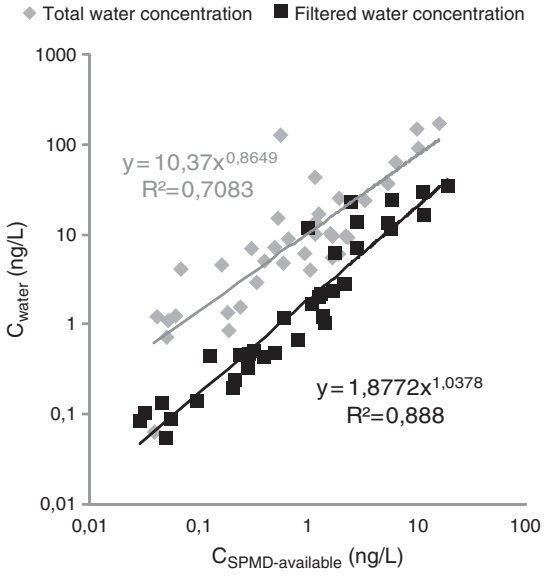

Fig. 3. Total and dissolved water concentrations against SPMD-available concentrations. Each point corresponds to the average value measured at a site over the 11-month campaign (n = 11). For total water concentrations, the values from months 0 to 5 were excluded.

The C_{total} estimations corrected by [*TOC*] did not yield a better correlation with $C_{SPMD\text{-}bioavailable}$ than the one obtained in Fig. 3 from raw data. On the contrary, the predicted concentrations do not match the measured concentrations. Indeed, the r^2 coefficient is 0.17 (data not shown). Thus, taking into account *TOC* variability in the river did not improve the prediction of total PAH concentration, contrary to what was proposed by Allan et al. (2009). As it stands, in a monitoring perspective, SPMD-available concentrations should not be used to calculate any total dissolved concentrations.

5.2. Does mussel contamination reflect water contamination? Potential use for biomonitoring

As a first approach, *BCF* and *BSAF* were calculated and expressed as a function of PAH hydrophobicity (i.e. the octanol–water partition coefficient K_{ow}) since this relationship was widely reported in the literature. This approach assumes that the bioaccumulation of PAHs results from an equilibrium partitioning between the environment and the organism. Hence, *BCF* and *BSAF* are assumed to depend solely on the substance and on the organism.

In the present study, a relationship could be observed between *BCF* (calculated from the measured dissolved PAH concentration) and hydrophobicity for log K_{ow} values lower than 5.5 (Fig. 4). However, above this value, log *BCF* values leveled off, suggesting that some additional factors influencing the partitioning processes were not being taken into account. Jonker and van der Heijden (2007) demonstrated that this cutoff for most hydrophobic compounds was an artifact caused on the one hand by non-equilibrium conditions and on the other hand by the binding of PAHs to DOC, which overestimates the concentration of dissolved bioavailable PAH. In the present field study, non-equilibrium conditions are the most likely cause of this cut-off, since *BCF* calculation based on $C_{SPMD\text{-}available}$ — which solely quantifies the truly dissolved concentration did not improve the correlation with log K_{ow} (Fig. 4).

An equilibrium is usually not reached, either because the environmental PAH concentrations vary over time or because the time it takes to reach it is longer than the deployment's duration (especially for the most hydrophobic compounds) (Jonker and van der Heijden, 2007). However, based on the elimination rate k_e measured by Fisher et al. (1993) for pyrene and B(*a*)P, the time it takes to reach 95% of the equilibrium in zebra mussels is respectively 13 days and 14 days; these compounds having a log K_{ow} of 5.3 and 6.35 respectively. The equilibration time is assumed to be longer for compounds with higher log K_{ow}. Since the most hydrophobic compound among the studied PAHs has

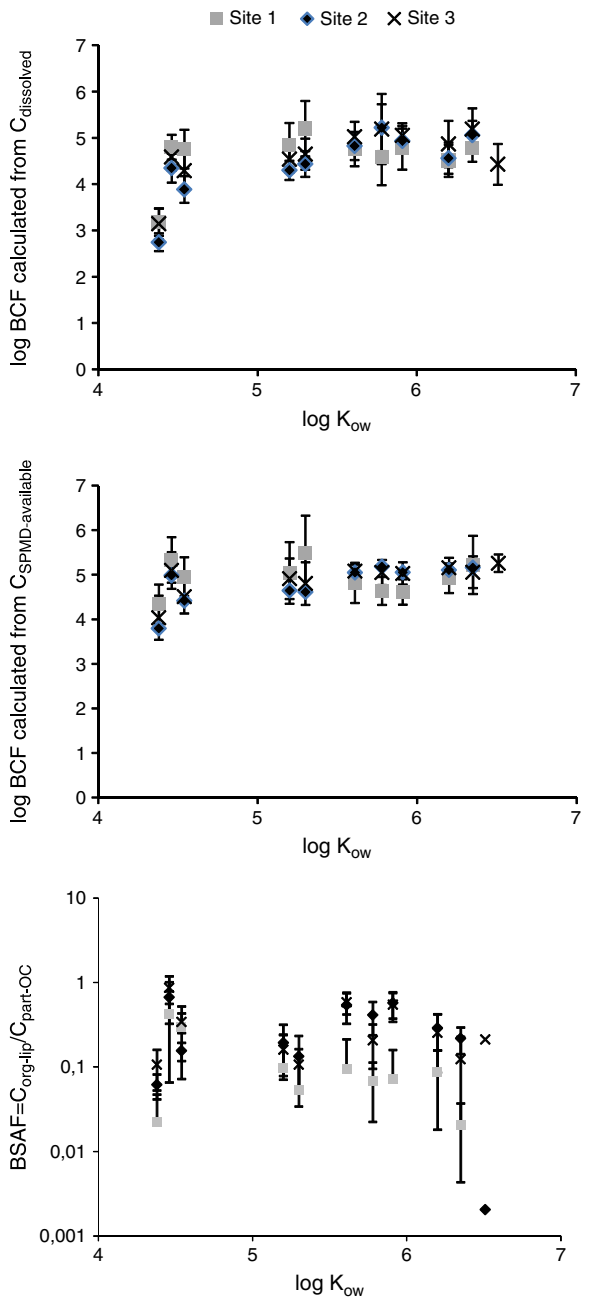

Fig. 4. Bioconcentration factor (*BCF*) calculated from either the dissolved or the SPMD-available concentration and biota-sediment accumulation factor (*BSAF*) for Sites 1, 2 and 3 as a function of log K_{ow}. C_{org_lip} is the lipid-adjusted concentration in organism and C_{part_OC} is the POC-adjusted concentration in particles. Each reported value is the mean over the 11-month exposure ± SD (n = 11).

a log K_{ow} of 6.9, its equilibration time should be similar to that of B(*a*)P (i.e. 14 days). Thus, the lack of equilibrium between water and mussels observed through *BCF* vs. log K_{ow} is probably due to the temporal variation of PAH exposure concentrations rather than to an insufficient duration of deployment.

Another hypothesis is that equilibrium partitioning models are inadequate for predicting the bioaccumulation of PAHs because complex biological processes occur. As can be observed in Fig. 4, lipid and POC normalizations were not useful in improving the correlation with log K_{ow}, which confirms the necessity of using a modeling tool to predict non-equilibrium PAH contents.

In the following we tested the predictive abilities of biodynamic modeling for pyrene. We first investigated the adequacy of the

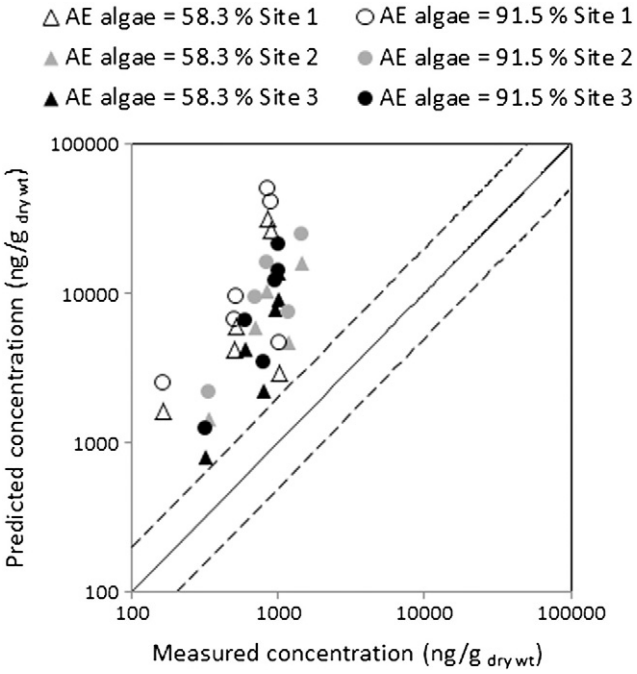

Fig. 5. Measured and predicted pyrene concentrations (ng $g^{-1}_{dry\ wt}$) as a function of the site and of the assimilation efficiencies determined by Gossiaux et al. (1998) for algae and sediment. Only the data for the last 6 months of exposure are shown since particulate PAH concentrations were not measured over the first 5 months.

biodynamic constants found in the literature (Gossiaux et al., 1998; Fisher et al., 1993) through a comparison of measured vs. predicted pyrene concentrations. The model strongly overestimated the pyrene concentrations in mussels, whichever AE is used — that measured in algae or in sediment (Fig. 5). Moreover, more than 96% of the pyrene is accumulated through the trophic pathway, which shows that the critical point to predict its bioaccumulation is not the dissolved exposure evaluation, but rather the trophic exposure or the elimination processes.

5.3. Insights into the mechanisms of uptake and loss

To better understand the mechanisms driving trophic contamination, AEs were determined for each site and date from the pyrene content actually measured in mussels. A temporal variation was clearly apparent (Fig. 6A). Surprisingly, AE was low before and after the spawning period (mean AE is 4% for all three sites) and higher during spawning (mean AE is 15%). This could be interpreted as resulting from a higher food requirement of mussels during this period, a greater uptake of nutriment leading to a greater uptake of contaminants. However, AE for metals determined in a conjoint study did not increase during spawning (Bourgeault et al., 2011), invalidating this initial interpretation.

Another hypothesis could be that greater lipid content in mussels enhances pyrene assimilation during spawning. However, the lipid content measured in the present study is stable over time, this hypothesis could not explain the variation of the predicted AE. Moreover, Bruner et al. (1994) have shown that, as far as dissolved uptake is concerned, the lipid content in zebra mussels does not influence the uptake kinetics of pyrene.

Another hypothesis, based on Dynamic Energy Budget (DEB) theory (Kooijman and Vanharen, 1990; Kooijman, 2000), is that the energy allocated for reproduction during spawning is not available for other purposes and more specifically for metabolic degradation of PAHs. Bustamante et al. (2012) have shown that the metabolization of pyrene in the oyster *Crassostrea gigas* is relatively weak. Nevertheless, McElroy et al. (2000) observed a high variability between species in their ability to metabolize PAHs and showed that molluscs may have a

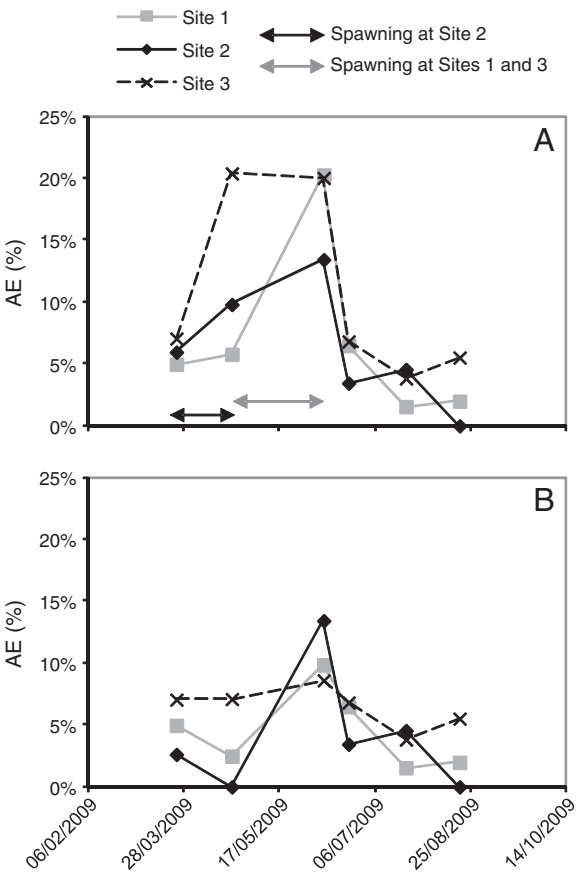

Fig. 6. Assimilation efficiency (AE) of pyrene by zebra mussels determined from the biodynamic model along the last 6 months of exposure, considering that the elimination rate (k_e) is either constant (A) or decreased by a factor of 2 during spawning (B).

strong metabolization system. In the present model, the elimination rate (which includes the rate constant for depuration via gills and feces and the biotransformation constant) was considered constant. Thus, the variation in the metabolic capacities of mussels depending on their biological state is not taken into account. However, an overestimation of k_e during spawning would lead to overestimated losses and would induce an overestimation of the predicted parameter — in this case AE. For pyrene, Bruner et al. (1994) reported a lower k_e for high-lipid pre-spawning mussels than for low-lipid post-spawning mussels, although this difference was not statistically significant. In order to investigate the effect of k_e variation on the resulting pyrene AE, we considered a case where k_e decreased by a factor of 2 during spawning. As shown in Fig. 6B, in this case, AEs remained roughly constant over the exposure, which confirmed that metabolization processes greatly impact the loss of PAHs and thus the models' predictions. Thanks to an increase of AE during spawning, the biodynamic model showed that the metabolization of pyrene most likely decreased during this period.

The major impact of mussel physiology on pyrene AE was confirmed with a Partial Least Squares (PLS) regression (XLStat 2010 4.03). PLS, a regression that is similar to PCA, is used to connect Y variables (in this case the response AE) to X variables (the predictors related to physicochemical and biological parameters). All data (reported on Table S1) were centered and scaled to unit variance. Despite a rather low goodness of fit ($r^2_X = 0.322$ and $r^2_Y = 0.477$) and goodness of prediction ($Q^2 = 0.315$) – Q^2 values usually reach 0.5 for a good model – the PLS analysis allowed us to disentangle the causal relationships between AE and the entire dataset. The PLS shows that the variables with the greatest influence on pyrene AE are the particulate concentration (C_{part}) and the physiological parameters (i.e. condition index, dry weight of mussels, ingestion rate and filtration rate) (Fig. S4).

6. Conclusion

In the present study, we analyzed the composition and level of PAHs in mussels exposed to low concentrations for 11 months. The relationship between PAHs in organisms and environmental concentrations cannot be described by *BCF* or *BSAF*, even if these factors are calculated from the SPMD-available concentrations. Indeed, models based on kinetic rather than simple equilibrium partitioning are more apt to interpret and predict PAH accumulation in mussels. The biodynamic model, in particular, points out the major impact of the biological cycle of mussels on their uptake and loss of PAHs, as well as the minor influence of site-specific environmental conditions. The temporal variation observed in the present study can likely be attributed to a less effective metabolization of PAHs, which in turn may be due to the energy costs of reproduction. A PLS analysis confirmed that physiological parameters were the most influential factors on the uptake/loss processes for pyrene. Since the biological state of mussels is a critical factor, SPMD passive samplers are not adequate to link organism and environment contaminations if the main purpose of the study is to assess PAH bioavailability throughout the year.

Acknowledgments

The authors thank L. Bervoets for providing the protocol for lipid extraction, as well as A. Germain and E. Uher for their support in the field work and sample analysis. This project received financial support from the Ile-de-France Regional Council (R2DS program) in the form of A. Bourgeault's PhD grant, as well as from the PIREN-Seine research program.

Appendix A. Supplementary data

Supplementary data to this article can be found online at http://dx.doi.org/10.1016/j.scitotenv.2013.03.021.

References

Allan I, Booij K, Paschke A, Vrana B, Mills GA, Greenwood R. Field performed of seven passive sampling devices for monitoring of hydrophobic substances. Environ Sci Technol 2009;43:5383–90.
Bayen S, Ter Laak TL, Buffle J, Hermens JLM. Dynamic exposure of organisms and passive samplers to hydrophobic chemicals. Environ Sci Technol 2009;43:2206–15.
Bervoets L, Voets J, Chu S, Covaci A, Schepens P, Blust R. Comparison of accumulation of micropollutants between indigenous and transplanted zebra mussels (*Dreissena polymorpha*). Environ Toxicol Chem 2004;23:1973–83.
Binelli A, Galassi S, Provini A. Factors affecting the use of *Dreissena polymorpha* as a bioindicator: the PCB pollution in Lake Como (N. Italy). Water Air Soil Pollut 2001;125:19–32.
Binelli A, Cogni D, Parolini M, Provini A. Multi-biomarker approach to investigate the state of contamination of the R. Lambro/R. Po confluence (Italy) by zebra mussel (*Dreissena polymorpha*). Chemosphere 2010;79(5):518–28.
Blasco C, Picò Y. Prospects for combining chemical and biological methods for integrated environmental assessment. TrAC Trends Anal Chem 2009;28(6):745–57.
Boehm PD, Page DS, Brown JS, Neff JM, Bence AE. Comparison of mussels and semi-permeable membrane devices as intertidal monitors of polycyclic aromatic hydrocarbons at oil spill sites. Mar Pollut Bull 2005;50:740–50.
Booij K, Zegers BN, Boon JP. Levels of some polybrominated diphenyl ether (PBDE) flame retardants along the Dutch coast as derived from their accumulation in SPMDs and blue mussels (*Mytilus edulis*). Chemosphere 2002;46:683–8.
Booij K, Smedes F, Honkoop PJC. Environmental monitoring of hydrophobic organic contaminants: the case of mussels versus semipermeable membrane devices. Environ Sci Technol 2006;40:3893–900.
Bourgeault A, Gourlay-Francé C, Vincent-Hubert F, Palais F, Geffard A, Biagianti-Risbourg S, et al. Lessons from a transplantation of zebra mussels in a small urban river: an integrated ecotoxicological assessment. Environ Toxicol 2010;25:468–78.
Bourgeault A, Gourlay-Francé C, Priadi C, Ayrault S, Tusseau-Vuillemin M-H. Bioavailability of particulate metal to zebra mussels: biodynamic modelling shows that assimilation efficiencies are site-specific. Environ Pollut 2011;159:3381–9.
Bruner KA, Fisher SW, Landrum PF. The role of the zebra mussel, *Dreissena polymorpha*, in contaminant cycling: I. The effect of body size and lipid content on the bioconcentration of PCBs and PAHs. J Great Lakes Res 1994;20:725–34.
bustamante p, luna-acosta a, clemens s, cassi r, thomas-guyon h, warnau m. Bioaccumulation and metabolisation of 14c-pyrene by the Pacific oyster *Crassostrea gigas* exposed via seawater. Chemosphere 2012;87:938–44.

Fisher S, Gossiaux D, Bruner K, Landrum P. Investigations of the toxicokinetics of hydrophobic contaminants in the zebra mussel (*Dreissena polymorpha*). Zebra mussels: biology, impacts, and control, vol. 28. Boca Raton, FL: Lewis Publishers; 1993. p. 465–90.

Gale RW, Huckins J, Petty JD, Peterman PH, Williams LL, Morse D, et al. Comparison of the uptake of dioxin-like compounds by caged channel catfish and semipermeable membrane devices in the Saginaw River, Michigan. Environ Sci Technol 1997;31: 178–87.

Gossiaux DC, Landrum PF, Fisher SW. The assimilation of contaminants from suspended sediment and algae by the zebra mussel, *Dreissena polymorpha*. Chemosphere 1998;36: 3181–97.

Gourlay C, Miege C, Noir A, Ravelet C, Garric J, Mouchel J-M. How accurately do semi-permeable membrane devices measure the bioavailability of polycyclic aromatic hydrocarbons to *Daphnia magna*? Chemosphere 2005;61:1734–9.

Gourlay-Francé C, Lorgeoux C, Tusseau-Vuillemin MH. Polycyclic aromatic hydrocarbon sampling in wastewaters using semipermeable membrane devices: accuracy of time–weight–average concentration estimations of truly dissolved compounds. Chemosphere 2008;73:1194–200.

Huckins JN, Manuweera GK, Petty JD, Mackay D, Lebo JA. Lipid-containing semipermeable membrane devices for monitoring organic contaminants in water. Environ Sci Technol 1993;27:2489–96.

Huckins JN, Petty JD, Booij K. Monitors of organic chemicals in the environment, semipermeable membrane devices. New York: Springer; 2006.

Jonker MTO, van der Heijden SA. Bioconcentration factor hydrophobicity cutoff: an artificial phenomenon reconstructed. Environ Sci Technol 2007;41:7363–9.

Kooijman SALM. Dynamic energy and mass budgets in biological systems. 2nd ed. Cambridge, UK: Cambridge University Press; 2000.

Kooijman S, Vanharen RJF. Animal energy budgets affect the kinetics of xenobiotics. Chemosphere 1990;21:681–93.

McElroy A, Leitch K, Fay A. A survey of in vivo benzo alpha pyrene metabolism in small benthic marine invertebrates. Mar Environ Res 2000;50:33–8.

Michel C, Bourgeault A, Gourlay-Francé C, Palais F, Geffard A, Vincent-Hubert F. Seasonal and PAH impact on DNA strand-break levels in gills of transplanted zebra mussels. Ecotoxicol Environ Saf in press. http://dx.doi.org/10.1016/j.ecoenv.2013.01.018.

Priadi C, Bourgeault A, Ayrault S, Gourlay-Francé C, Tusseau-Vuillemin MH, Bonté P, et al. Spatio-temporal variability of solid, total dissolved and labile metal: passive vs discrete sampling evaluation in river metal monitoring. J Environ Monit 2011;13:1470–9.

Roper JM, Cherry DS, Simmers JW, Tatem HE. Bioaccumulation of PAHs in the zebra mussel at Times Beach, Buffalo, New York. Environ Monit Assess 1997;46:267–77.

Schwarzenbach R, Gschwend PM, Imboden DM. Environmental organic chemistry. New York, USA: John Wiley & Sons; 1993.

Tusseau-Vuillemin MH, Gourlay C, Lorgeoux C, Mouchel JM, Buzier R, Gilbin R, et al. Dissolved and bioavailable contaminants in the Seine river basin. Sci Total Environ 2007;375:244–56.

Verweij F, Booij K, Satumalay K, van der Molen N, van der Oost R. Assessment of bioavailable PAH, PCB and OCP concentrations in water, using semipermeable membrane devices (SPMDs), sediments and caged carp. Chemosphere 2004;54:1675–89.

Voets J, Talloen W, de Tender T, van Dongen S, Covaci A, Blust R, et al. Microcontaminant accumulation, physiological condition and bilateral asymmetry in zebra mussels (*Dreissena polymorpha*) from clean and contaminated surface waters. Aquat Toxicol 2006;79:213–25.

Wang W-X, Rainbow PS. Comparative approaches to understand metal bioaccumulation in aquatic animals. Comp Biochem Physiol C 2008;148:315–23.